International Telecommunication Union

ITU-R

Radiocommunication Sector of ITU

Report ITU-R SM.2355-1

(06/2019)

Spectrum monitoring evolution

SM Series

Spectrum management

Foreword

The role of the Radiocommunication Sector is to ensure the rational, equitable, efficient and economical use of the radio-frequency spectrum by all radiocommunication services, including satellite services, and carry out studies without limit of frequency range on the basis of which Recommendations are adopted.

The regulatory and policy functions of the Radiocommunication Sector are performed by World and Regional Radiocommunication Conferences and Radiocommunication Assemblies supported by Study Groups.

Policy on Intellectual Property Right (IPR)

ITU-R policy on IPR is described in the Common Patent Policy for ITU-T/ITU-R/ISO/IEC referenced in Resolution ITU-R 1. Forms to be used for the submission of patent statements and licensing declarations by patent holders are available from http://www.itu.int/ITU-R/go/patents/en where the Guidelines for Implementation of the Common Patent Policy for ITU-T/ITU-R/ISO/IEC and the ITU-R patent information database can also be found.

Series of ITU-R Reports

(Also available online at http://www.itu.int/publ/R-REP/en)

Series	Title
BO	Satellite delivery
BR	Recording for production, archival and play-out; film for television
BS	Broadcasting service (sound)
BT	Broadcasting service (television)
F	Fixed service
M	Mobile, radiodetermination, amateur and related satellite services
P	Radiowave propagation
RA	Radio astronomy
RS	Remote sensing systems
S	Fixed-satellite service
SA	Space applications and meteorology
SF	Frequency sharing and coordination between fixed-satellite and fixed service systems
SM	**Spectrum management**

***Note**: This ITU-R Report was approved in English by the Study Group under the procedure detailed in Resolution ITU-R 1.*

Electronic Publication
Geneva, 2019

REPORT ITU-R SM.2355-1

Spectrum monitoring evolution

(2015-2019)

TABLE OF CONTENTS

Page

1 Introduction

The goal of spectrum management is to maximize spectrum efficiency, minimize interference and eliminate unauthorized and improper use of the spectrum. As the eyes and ears of the spectrum management process, spectrum monitoring is very necessary and important in the management of spectrum resources, radio stations of various types, and the electromagnetic environment by providing valuable monitoring data, including spectrum occupancy and characteristics of signals, such as field strength, bandwidth, modulation type, locations of emitters, etc.

Radiocommunication systems are in a constant and rapid evolution. With respect to spectrum utilization, new technologies in radiocommunication systems may include adaptive frequency usage, co-frequency multiplexing, wideband access, spread spectrum (direct sequence spread spectrum and frequency hopping), etc. Software-defined radio and cognitive radio are typical examples for new radiocommunication systems. Correspondingly, future spectrum monitoring systems should have the capability for monitoring new radiocommunication technologies and systems, such as detection of weak signals, co-frequency signal separation and multi-mode location based on digital signal processing (DSP), RF sensor networking, and other technologies.

2 Detection of weak signals

It is necessary to improve the sensitivity of monitoring systems for the detection of weak signals with low-power-density because many new radiocommunication systems are running with lower power, wider bandwidth and higher frequencies.

In some circumstances, signals may be weaker than the background noise. Consequently, it is difficult to detect and locate illicit low-power-density weak signals using existing low sensitivity monitoring systems. Future spectrum monitoring systems should use advanced technologies to extract signals from background noise.

Several technologies can be used for the detection of weak signals and are listed in the following sections.

2.1 Locked-in amplifier

A locked-in amplifier (LIA) uses a reference signal to extract a signal with known or expected internal parameters from a noisy environment.

The sine wave is the most common signal among data communication signals and its amplitude and phase can be estimated by the locked-in amplifier. Assuming the received signal is:

$$x(t) = U_s \cos \omega_0 t + n(t) \quad (1)$$

where:

U_s: amplitude of the sine wave signal

w_0: angular frequency

$n(t)$: background noise.

U_s could be estimated by cross-correlation of the received signal and the local reference signal, as shown in Fig. 1.

FIGURE 1

Diagram of LIA

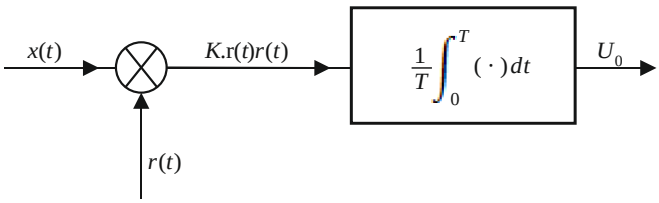

Report SM.2355-0

In Fig. 1, $r(t)$ is a reference signal with amplitude U_r and phase φ. The frequency of $r(t)$ is the same as $x(t)$. K is a constant associated with the multiplier. The output U_0 could be described as:

$$Uo = \lim_{T\to\infty} \frac{1}{T}\int_0^T K[U_s \cos w_0 t + n(t)][U_r cos(w_0 t + \phi)]dt \tag{2}$$

Since the background noise is irrelevant to the sine wave signal, the additive noise in (2) is ignored and it can be written as follows:

$$U_0 = \frac{KU_sU_r}{2}\cos\varphi \tag{3}$$

Apparently, U_0 would get the maximum value when φ is zero and U_s can therefore be obtained accurately. In this situation, the reference signal $r(t)$ and the received signal $x(t)$ have the same phase.

Above, it is shown that LIA is essentially the application of the cross-correlation between received signal and local reference signal. The key issue for the LIA above is the recovery of frequency and phase of the reference signal, which can be achieved through phase-locked loop circuits.

2.2 Correlation

2.2.1 Cross-Correlation

Cross-correlation is a measure of the similarity of two waveforms as a function of a time-lag applied to one of them. It is assumed that

$$x(t) = s_1(t) + n_1(t), \qquad y(t) = s_2(t) + n_2(t) \tag{4}$$

and then

$$\begin{aligned} R_{xy}(\tau) &= E[y(t)x(t-\tau)] = E\{[s_2(t) + n_2(t)][s_1(t-\tau) + n_1(t-\tau)]\} \\ &= R_{s_1s_2}(\tau) + R_{s_1n_2}(\tau) + R_{n_1s_2}(\tau) + R_{n_1n_2}(\tau) = R_{s_1s_2}(\tau) \end{aligned} \tag{5}$$

is the ensemble average operator comprising the average over several data samples.

If assuming $x(t)$ as a predetermined sequence in the receiver, then the cross-correlation can be used to detect the received signal $y(t)$ even if $y(t)$ is weaker than the background. This is because the purpose of cross-correlation in this case is to find a predetermined pattern in the received sequence, which is usually a pseudo random noise sequence. We can only observe a peak when the desired signal in the received signal is aligned to the predetermined sequence. This principle has been used for weak signal detection in DSSS system (Direct sequence spread spectrum).

2.2.2 Auto-Correlation

Auto-correlation is the cross-correlation of a signal with itself. If assuming $x(t) = s(t) + n(t)$, when $s(t)$ is periodical signal, and n(t) is the noise. Then, the auto-correlation can be defined as

$$\begin{aligned} R_x(\tau) &= E\left[x(t)x(t-\tau)\right] = E\left\{\left[s(t)+n(t)\right]\left[s(t-\tau)+n(t-\tau)\right]\right\} \\ &= E\left[s(t)s(t-\tau)\right]+E\left[n(t)n(t-\tau)\right]+E\left[s(t)n(t-\tau)\right]+E\left[n(t)s(t-\tau)\right] \\ &= R_s(\tau)+R_n(\tau)+R_{sn}(\tau)+R_{ns}(\tau) \end{aligned} \tag{6}$$

If s(t) and n(t)are not correlated, we have

$$R_{sn}(\tau) = R_{ns}(\tau) = 0 \qquad R_x(\tau) = R_s(\tau) + R_n(\tau) \tag{7}$$

If the noise signal n(t) is not periodical and its average value is zero, then:

$$R_n(\tau) = 0 \text{ (where } \tau \neq 0) \tag{8}$$

Thus

$$R_x(\tau) = R_s(\tau)$$

Auto-correlation is useful for weak signal detection. Informally, auto-correlation can be viewed as searching the similarity between different observations of a same signal. Apparently, such similarity can only occur for the desired signal, which has pre-designed format including periodical feature. Additive noise can hardly generate such similarity between different observations. In this way, the impact caused by strong additive noise can be alleviated effectively.

2.3 Higher Order Statistics (HOS)

In statistical analysis of signals, the mean and the correlation (auto and cross) of the signals are known as the first and second moments respectively. The spectrum monitoring techniques reported earlier in this study are based on either the first order moment or the second moment (Locked In amplifier, § 2.1). However, there is much more information in a communication or radar signals than is conveyed by the first and second moments and their associated spectral values. Among this information are signal phase, non-linearity, non-Gaussian noise, symmetry, etc. HOS has been widely used in eliminating Gaussian noise, detecting non-Gaussian signals, detecting signal non-linearity, detecting transient signals, etc.

As mentioned above HOS is based on the following variables:

– Poly-spectra
– Higher-order moments
– Cumulants.

The most used of those variables are the third moment, the fourth moment, the bi-spectrum, and the tri-spectrum.

Figures 2 and 3 below are calculated to illustrate how the phase information is preserved by HOS variables. Both Figures show the bi-spectrum of a rectangular pulse modulated by a carrier cosine wave ($\cos(2\pi f_c + \varphi_0)$), where f_c is the carrier frequency, and φ_0 is the carrier phase. In Fig. 2, the carrier phase is taken to be 0°, and in Fig. 3, the carrier phase is taken to be 45°. Comparing Fig. 2 against Fig. 3 indicates that phase values φ_0 are reflected into both the level and trend of the bi-spectrum. Accordingly, bi-spectrum data could be exploited in extracting signal phase values.

FIGURE 2

The bi-spectrum of a rectangular pulse modulated by a carrier cosine wave (f_c = 2, and φ_0 = 0°)

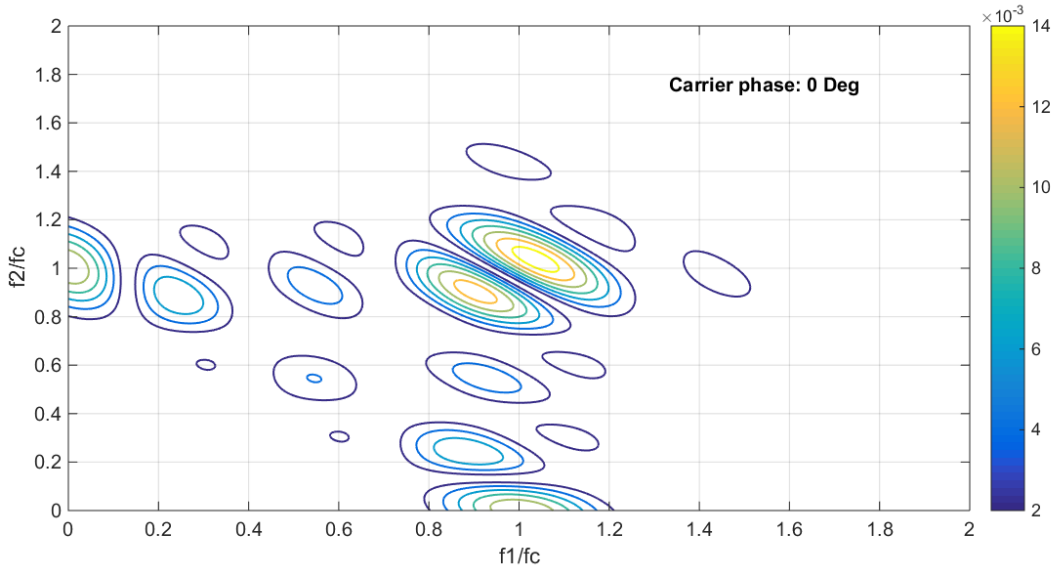

FIGURE 3

The bi-spectrum of a rectangular pulse modulated by a carrier cosine wave (f_c = 2, and φ_0 = 45°)

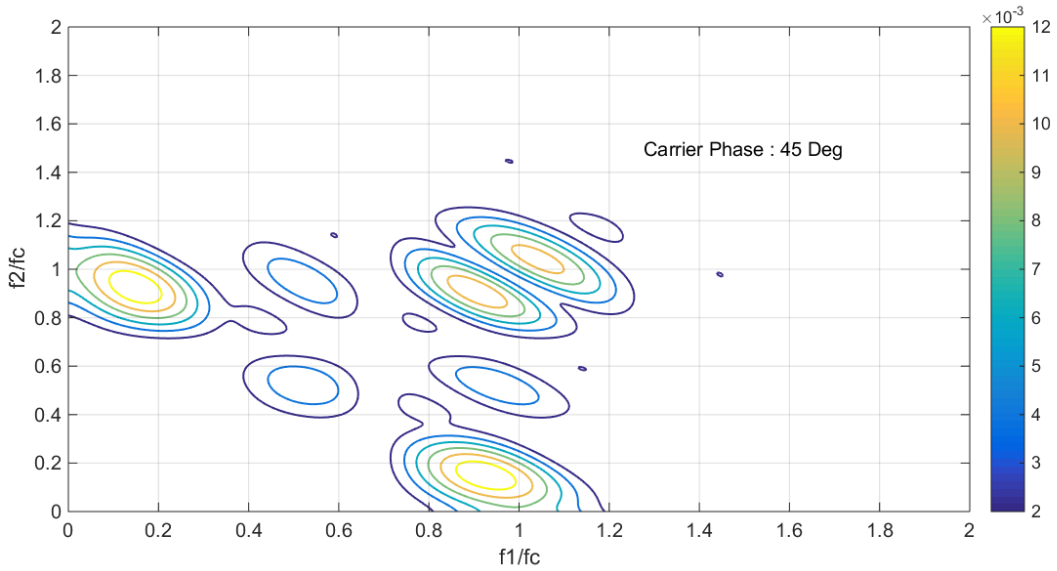

It should be mentioned that, similar to cross correlation, the higher order moments could also be performed on two or more different signals. In this case, spectrum, bi-spectrum, and tri-spectrum, are called cross spectrum, cross bi-spectrum, and cross tri-spectrum, respectively.

As a conclusion to this section, HOS is useful for weak signal detection because the bi-spectrum and tri-spectrum of additive noise, which is usually Gaussian distributed, can be zero. Since the HOS of desired signal is, in general, not zero, the additive noise in the received signal can be completely removed if taking the HOS of the received signal. In this manner, the additive noise is cancelled and signal weaker than the background noise can be detected.

2.4 Cyclostationarity

The cyclostationarity principle takes advantage of signals that have statistical properties that vary cyclically with time. Many communication signals in use today may be modelled as cyclostationary signals due to the presence of one or more underlying periodicities which arise due to the coupling of stationary message signals with periodic sinusoidal carriers, pulse trains or repeating codes. Those underlying periodicities may also occur as a result of other processes used in the generation of the signal sampling and multiplexing.

Due to underlying periodicities, the autocorrelation function could be represented by a Fourier series on which the cyclostationary signature of signals is built as follows. For an underlying periodicity with a period T_0, the auto-correlation function could be expanded into Fourier series with respect to cyclic frequencies α (α = *m*/*T*, m = 0,1,2,...):

$$R_{xx}(t, t-\tau) = \sum_{\alpha} R_{xx}^{\alpha}(\tau) exp(j2\pi\alpha t/T_0) \quad (9)$$

The Fourier coefficients of the autocorrelation (9) give the cyclic autocorrelation function $R_{xx}^{\alpha}(\tau)$.

Fourier transform of the cyclic autocorrelation function (9) yields the spectral correlation density $S_{xx}^{\alpha}(f)$:

$$S_{xx}^{\alpha}(f) = \int_{-\infty}^{\infty} R_{xx}^{\alpha}(f)\, exp(-j2\pi f\tau) d\tau \quad (10)$$

The above spectral correlation density SCD could be considered as a generalization for the conventional power spectral density. Such a generalization stems from making SCD as a function of two frequencies: spectral frequency f and the cyclic frequency α/T_0 while PSD is function of the spectral frequency f only.

As a conclusion to this section, it should be mentioned that the cyclostationary-based detection is applicable to wide variety of wireless standards including CDMA and OFDM signals. Furthermore, there is a potential of enhancing the performance of the weak signal detection method through using cyclostationary features. This is because the additive noise has no cyclostationary feature and thus the spectral correlation density with non-zero cyclic frequency is zero. It means the additive noise in the received signal can be removed if using equation (9) to the received signal. In this manner, the additive noise can be cancelled and signal weaker than the background noise can be detected.

2.5 Adaptive noise cancelling

Adaptive noise cancelling (ANC) obtains the desired signal by subtracting adaptively filtered "reference" noise correlated with the noise contained in the detected signal from the detected signal.

The diagram of adaptive noise cancelling is shown in Fig. 4.

FIGURE 4

Diagram of ANC

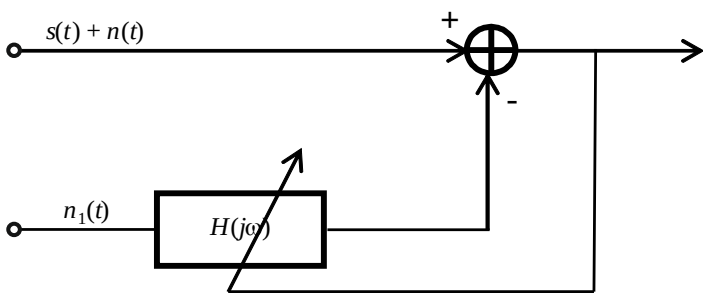

Report SM.2355-0

The reference noise $n_1(t)$ which is correlated with noise $n(t)$ could be processed by the adaptive filter $H(jw)$. The noise $n(t)$ could be suppressed, and the output SNR can be improved.

This ANC filter could be designed easily without knowledge or experience of the noise $n(t)$ and the signal $s(t)$, and the filtering effect is equivalent to the Wiener Filter. Because of its advantages, the ANC filter has been widely used to suppress the interference combined with the signals, e.g. the adaptive notch filter.

2.6 Summary

To improve the detection performance of weak signals, several detection algorithm types are investigated in the forgoing section. All involve some signal processing, but as shown above, some are more computationally intensive, and in some cases, there are trade-offs between computation time, signal duration and noise levels. Some techniques are effective on certain types of signals, while other techniques can be used for many types of signals.

3 Co-frequency signal separation

In order to share limited spectrum resources, more and more radiocommunication systems are working at the same frequency. For example, many kinds of cellular communication systems and HF communication systems are using co-frequencies. Meanwhile, many intended or unintended interference may occur at overlapping frequencies.

Co-frequency multiplexing techniques are adopted by many radiocommunication systems. In such cases, one spectrum monitoring station may receive many signals from different transmitters working at the same frequency. Consequently, it is difficult to differentiate these co-frequency signals using existing monitoring systems. Therefore, future spectrum monitoring systems should employ advanced technology for signal separation.

The technologies of co-frequency signal separation can be divided into two categories: single-channel separation and multi-channel separation, which are listed in the following sections.

3.1 Single-channel separation (Strong-signal recovery)

When there is only one receive channel, strong-signal recovery can be used to recover a signal from linear digital modulated signals, such as PSK and QAM modulated. However, this algorithm can only work in the case of two signals, and requires a power ratio of more than 6 dB. A diagram of this algorithm is shown in Fig. 5.

FIGURE 5

Diagram of strong-signal recovery

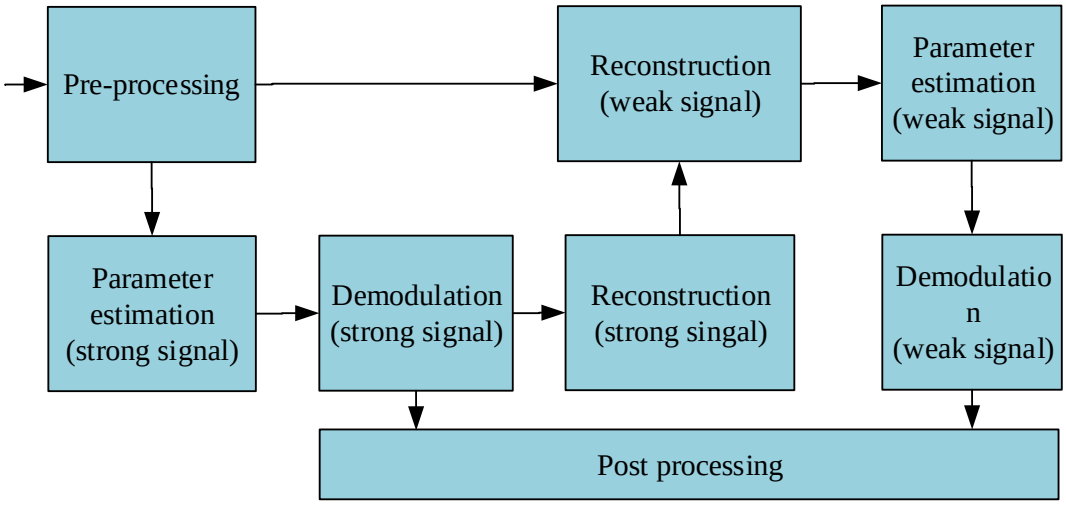

a) Pre-processing

The main function of this module includes several necessary receiving processing steps, such as filtering, down-conversion, sample rate conversion. Meanwhile, some narrow-band interference cancellation algorithms, such as adaptive notch filtering (which can eliminate the comparable weak signal added on the strong legal signal) can be applied to this module using frequency domain based algorithms.

b) Parameter estimation for strong signal

Several parameters should be estimated for demodulation of the strong signals in this module. These parameters include amplitude, carrier frequency, initial phase, modulation rate and type. However, in most cases, the strong signal is legal. Thus some inherent parameters, such as modulation rate and type, are known to the receiver. So there is no need to estimate these parameters. Only carrier frequency, initial phase and the amplitude needs to be estimated.

c) Demodulation and reconstruction of the strong signal

The conventional demodulation procedure can be used for the demodulation of strong signals to recover the bit stream sequence. Then the procedure of the strong signal reconstruction can be implemented with prior knowledge of carrier frequency, initial phase, baud rate and modulation type.

d) Reconstruction of the weak signal

After recovery of the strong signal, the weak signal can be reconstructed by adaptive signal cancellation techniques such as least mean square (LMS) and recursive least square (RLS) to eliminate the strong signal from the original mixed signal.

e) Parameter estimation for the weak signal

The required parameters are similar to those mentioned in section b). However, the characteristics of the interfering signal are unknown to the receiver, and thus the necessary parameters, such as baud rate and modulation type, should also be estimated. It is suggested that some robust parameter estimation algorithm should be introduced to eliminate the effect of inaccuracy of the reconstruction.

For instance, the cyclic-spectrum based algorithm can be applied to baud rate estimation, and some high-order statistics based algorithms can be used to design the modulation identification algorithm.

f) Demodulation of weak signal

As with the aforementioned statement in section b), the conventional demodulation method can be introduced for the weak signal. Meanwhile, it is suggested that a blind equalization step can be introduced to overcome the inter-symbol interference, which is generated from the inaccuracy of parameter estimation.

3.2 Multi-channel separation (Spatial spectrum based beam-forming)

Spatial spectrum based beam-forming can be used when there are multiple channels. It is especially suitable for the application in the scenario of the blind separation of multiple signals, which is also effective under arbitrary modulation types, and can achieve relatively good performance in low SNR environments. The basic theory can be illustrated as follows:

Assume *P* signals are received by *M* arrays, the received signals can be expressed by matrix $\boldsymbol{X}(t)$ as:

$$\boldsymbol{X}(t)=\begin{bmatrix} 1 & 1 & \cdots & 1 \\ e^{j2\pi d\sin\theta_1/\gamma} & e^{j2\pi d\sin\theta_2/\gamma} & \cdots & e^{j2\pi d\sin\theta_P/\gamma} \\ \vdots & \vdots & \ddots & \vdots \\ e^{j2\pi d(M-1)\sin\theta_1/\gamma} & e^{j2\pi d(M-1)\sin\theta_2/\gamma} & \cdots & e^{j2\pi d(M-1)\sin\theta_P/\gamma} \end{bmatrix}\begin{bmatrix} s_1(t) \\ s_2(t) \\ \vdots \\ s_P(t) \end{bmatrix}+\begin{bmatrix} n_1(t) \\ n_2(t) \\ \vdots \\ n_M(t) \end{bmatrix} \tag{11}$$

where $\{\theta_1,...\theta_P\}$ is the direction of each signal respectively, $s_i(t)$ $\{i = 1,2,...P\}$ denotes the *P* input signals, $n_i(t)$ $\{i = 1,2,...M\}$ is the corresponding additive white Gaussian noise (AWGN), and γ is the wavelength of the signal.

Then by calculating the correlation matrix, the following can be obtained:

$$\boldsymbol{R}=E\left(\boldsymbol{X}(t)\boldsymbol{X}^H(t)\right) \tag{12}$$

Applying an eigenvalue decomposition to (12), eigenvalues and eigenvectors can be obtained. The signal space can be divided into a P-dimensional signal subspace and a *M-P* dimensional noise subspace. Since the signal subspace and the noise subspace are orthogonal, the following can be obtained:

$$\boldsymbol{a}(\theta_k)\boldsymbol{G}\boldsymbol{G}^H\boldsymbol{a}^H(\theta_k)=0 \tag{13}$$

where $(\theta_k)=\left[1e^{j2\pi d\sin\theta_k/\gamma}...e^{j2\pi d(M-1)\sin\theta_k/\gamma}\right]^T$, $\boldsymbol{G}$ is composed of eigenvectors in noise subspace with dimension $M \times (M\text{-}P)$. By defining $\boldsymbol{P}(\theta) = 1/[\boldsymbol{a}(\theta_k)\boldsymbol{G}\boldsymbol{G}^H\boldsymbol{a}^H(\theta_k)]$, the direction of each signal can be obtained by peak-picking over $P(\theta)$. This is the well-known MUtiple SIgnal Classification (MUSIC) algorithm.

If the signal from direction θ_k is to be separated, the coefficients of each array should satisfy:

$$\boldsymbol{\omega}^H\boldsymbol{a}(\theta_d)=1,\ \ \boldsymbol{\omega}^H\boldsymbol{a}(\theta_i)=0\ \ (i=1,2,...,M, i\neq d) \tag{14}$$

Many algorithms can be used to solve the above problem. One of the most typical and widely used algorithm is the so-called “Capon beam forming”, which is designed to minimize the output power. The coefficients can be solved as:

$$\omega_{opt}=\left[R^{-1}a(\theta_k)\right]/\left[a^H(\theta_k)R^{-1}a(\theta_k)\right] \tag{15}$$

For frequency estimation in an undamped, superimposed exponential model, better results can be obtained using both the ordinary and the conjugate data than using only the ordinary one, although they are asymptotically equivalent. Therefore, a modified MUSIC (MMUSIC) algorithm is

proposed using both ordinary and conjugate data to estimate DOA of signals. Compared with the MUSIC algorithm, the correlation matrix of the MMUSIC is expressed as:

$$\overline{\boldsymbol{R}} = \boldsymbol{R} + \boldsymbol{J}E\left(\overline{\boldsymbol{X}}(t)\overline{\boldsymbol{X}}^{H}(t)\right)\boldsymbol{J} \tag{16}$$

where, $\overline{\boldsymbol{X}}(t)$ is the conjugate data of $\boldsymbol{X}(t)$, $\boldsymbol{J}$ is the $P \times P$ exchange matrix whose entries all are zero except the ones at the $(i, P - i + 1)$-th entry for $i = 1,2,...P$.

3.3 Summary

To achieve signal separation on the same frequency band, two co-frequency signal separation approaches are investigated in this section, including the single-channel approach and the multi-channel approach. The single-channel approach needs demodulation of the strong signal and thus causes more computational burden, while the multi-channel approach has no requirement of signal demodulation but needs more channels and corresponding antennas for signal separation.

4 Multi-mode location (based on a combination of location technologies)

Signals in different domains carry related location information. Correspondingly, such location information can be extracted by corresponding technology or computer processing algorithms. Digital signal processing (DSP) and networking capability is becoming more and more powerful. Devices based on DSP and networking are becoming more affordable. Spectrum-monitoring systems based on DSP algorithms and network technology can make identification of transmitters with different characteristics working in different domains easier, including amplitude domain, frequency domain, time domain, spatial domain, code domain, etc. Consequently, multi-mode location technology may be used to locate emitters under different circumstances based on combination of different location technologies, such as AOA (angle of arrival), TDOA (time difference of arrival), FDOA (frequency difference of arrival), POA (power of arrival), and identification data-aided techniques.

4.1 Angle of arrival

Angle of arrival (AOA) is a traditional and popular method of locating a transmitter by determining the direction of propagation of a wave incident on an antenna array under many circumstances. There are many techniques to find the bearing, such as phase interferometer, correlative interferometer, mono pulse techniques, beam forming and space matched filter, subspace techniques, etc. For certain applications, some techniques may be combined in one DF monitoring station for different purposes. In order to locate a transmitter, it is necessary to combine the results from two or more DF monitoring stations to obtain a cross-bearing based on AOA technology.

4.2 Time difference of arrival

Time difference of arrival (TDOA) is one promising method of locating a transmitter by estimating the difference in the arrival times of the signal from the source at multiple receivers. TDOA systems offer flexibility in antenna selection and placement as TDOA accuracy is minimally affected by nearby reflectors. In order to locate a transmitter, it is necessary to combine three or more TDOA systems deployed at different sites. Based on the TDOA values of different pairings of receivers, the position of a transmitter may be determined by utilizing some algorithms, such as non-iterative and iterative algorithms. A more complete discussion of TDOA methods is contained in the Report ITU-R SM.2211.

4.3 Frequency difference of arrival

Frequency difference of arrival (FDOA) is one effective method for locating a transmitter in motion or locating a transmitter by a mobile monitoring station, especially an airborne one. Rapid switch among the receive antennas of a monitoring antenna array has a similar effect to that caused by relative motion between transmitter and monitoring receiver. Since the relative motion can be used to obtain the transmitter location via Doppler estimation, TDOA and FDOA can then be used together to improve location accuracy and the resulting estimates are somewhat independent. By combining TDOA and FDOA measurements, instantaneous geolocation can be performed in two dimensions.

4.4 Power of arrival

Power of arrival (POA) is one economical method of locating a transmitter because POA does not require additional monitoring receiver hardware. The power of a radio signal can be estimated according to propagation models with the knowledge of transmitter power and propagation path, which is especially useful for standardized wireless communication systems. However, it cannot be used to locate a transmitter when transmitter power is unknown. In some circumstances, it is easy to locate a transmitter when propagation model is simple, e.g. locating an FM broadcasting transmitter when LOS propagation exits between FM broadcasting transmitter and fixed monitoring stations.

4.5 ID-Aided

ID-Aided is a more and more important method for locating a transmitter used as a sensor in such a new era of global interconnectedness, especially for pubic radiocommunication networks. Digitalized radiocommunication system includes additional information of user identification, which can be used to obtain the transmitter information, such as longitude and latitude, IP address, etc. It is more effective to locate a transmitter with combinational information from monitoring station and matched radiocommunication network database when the transmitter is operating for mobile services. Satellite mobile phone, satellite Internet terminal and handset mobile phone are classical transmitter which could be located by using the ID-Aided method.

4.6 Summary

Multi-mode location is basically a combination of different location approaches. This section investigates different location approaches, including AOA based, TDOA based, FDOA based, POA based and ID-Aided. Some approaches have no requirement of the information carried by the signal, while other methods have to recover the information carried by the signal for location, which will increase the computational burden.

5 Conclusion

The techniques and applications for detection of weak signal, co-frequency signal separation and multi-mode location based on DSP and network are briefly described in this Report, including locked-in amplifier, correlation, HOS, cyclostationary, adaptive noise cancelling, strong signal recovery, spectrum-based beam-forming, TDOA, FDOA, POA, and ID-Aided, which may be used in future spectrum monitoring under different circumstances.

More advanced spectrum monitoring techniques and applications should be studied for implementation in order to respond to the rapid development of new radiocommunication systems. Examples of some advanced monitoring techniques are found in Annexes 1 and 2.

Annex 1

Examples of the application of advanced monitoring techniques

A1.1 Correlation application in satellite interference finding

In many cases, GSO satellite interference can be located within an ellipse area whose centre is tens of kilometres or farther from the transmitter location.

In the above circumstance, signals from the interfered satellite and adjacent satellite are correlated by the transmitter location systems, and then the TDOA and FDOA data can be generated.

To quickly locate and identify transmitter on the ground is a key issue by spectrum-monitoring stations in many countries or administrations.

The weak signal transmitted by side-lobes of an antenna, which points to GSO satellite, should be detected by equipment. Then we can utilize the cross-correlation technique to improve the sensitivity of the monitoring system installed on the mobile vehicle. A brief diagram of this application is shown in Fig. A1-1.

FIGURE A1-1

Diagram of cross-correlation application in satellite interference finding

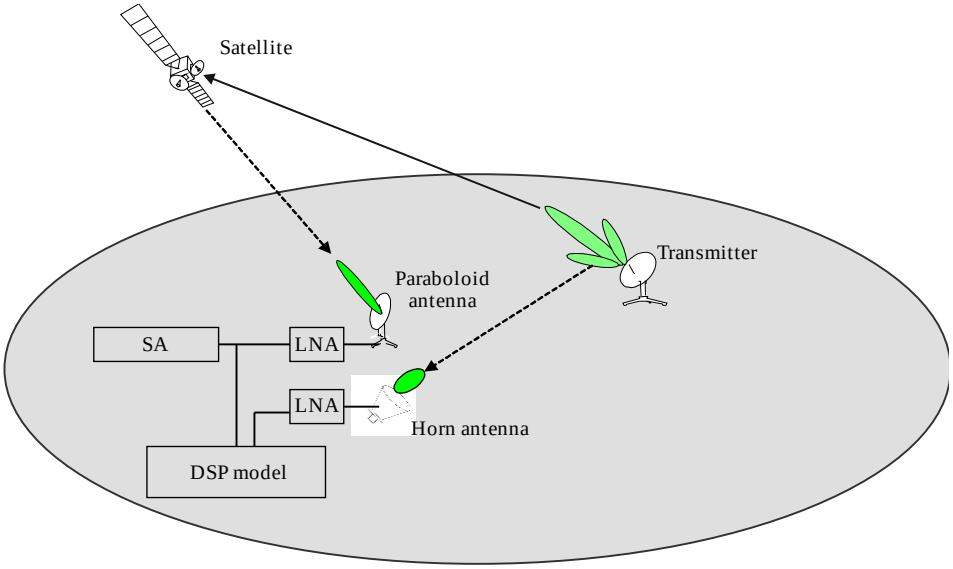

Report SM.2355-A1-0

In this system, cross-correlation arithmetic is utilized in the DSP module to process signals from the satellite by parabolic antenna and from the side-lobe of the earth station antenna by horn antenna or isotropic antenna directly.

The process diagram in the DSP module is described in Fig. A1-2.

FIGURE A1-2

Process diagram in DSP module

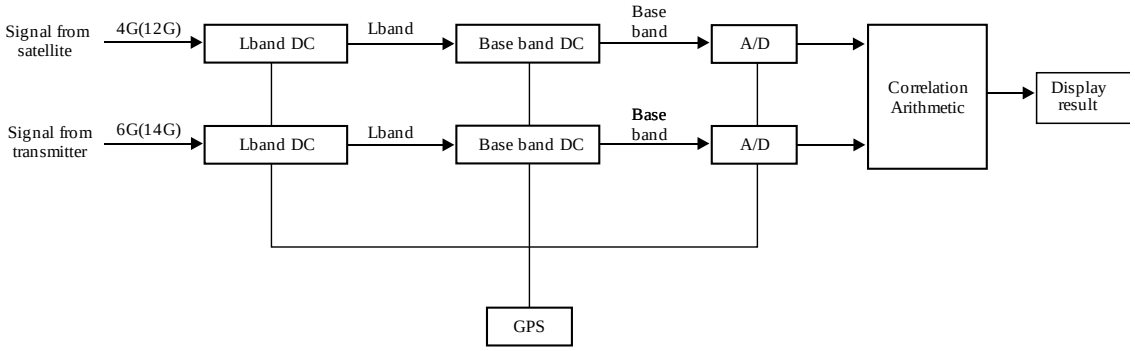

Report SM.2355-A1-0

In the cross-correlation arithmetic, the complex ambiguity function based on a second-order statistics (CAF-SOS) algorithm is used to simultaneously estimate the TDOA and FDOA of signals from satellite and transmitter.

The cross-correlation SNR can be described as follows and each *snr* is a linear value.

$$snr = 2BT * \frac{snr_1 * snr_2}{1 + snr_1 + snr_2}$$

Where $2BT$ is processing gain, if signals are sampled with the Nyquist rate and N is the sample point number, we shall get $2BT = N$. The snr_1 represents the snr of signal from satellite, and snr_2 represents the snr of the signal from transmitter. In common cases, *snr* is no less than 20 dB.

If *snr* is equal to 10 dB, the relation between *snr* and snr_2 can be described as in Fig. A1-3.

FIGURE A1-3

Relation between *snr* and snr_2 when snr_1 = 10 dB

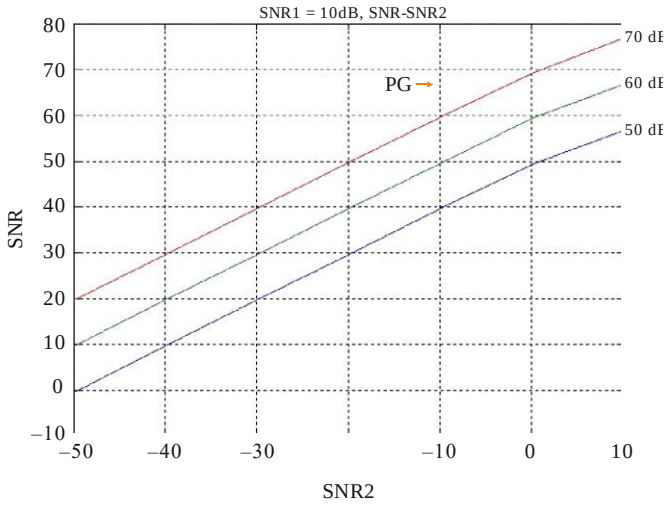

Report SM.2355-A1-03

Typically, the equipment using cross-correlation arithmetic can detect weak signals with about −40 dB snr value if the processing gain is 60 dB. That is to say, it can capture the weak signal with a power spectrum density 40 dB lower than the noise floor.

In practice, the directional horn antenna rotates by a certain angle followed by a cross-correlation process. After rotating 360 degrees, the operator would be able to find the direction of the

transmitter when the correlation snr of the both channels (from satellite and from earth station) maximizes, even when the level of the terrestrial signal is too weak to be observed with a spectrum analyser (see Fig. A1-4).

FIGURE A1-4

Peak angle graph

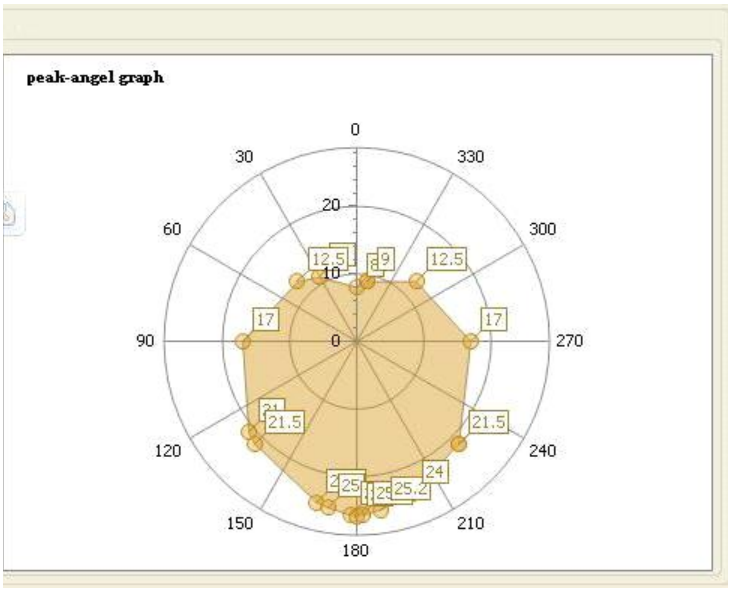

Report SM.2355-A1-0

Alternately, equipment using cyclic auto-correlation based arithmetic can detect weak signals with about –20 dB snr values, correspondingly. Although the performance is worse than cross-correlation based arithmetic, it still exhibits better sensitivity than traditional FFT-based detection algorithm. The diagram is shown in Fig. A1-5.

FIGURE A1-5

Diagram of cyclic auto-correlation application in satellite interference finding

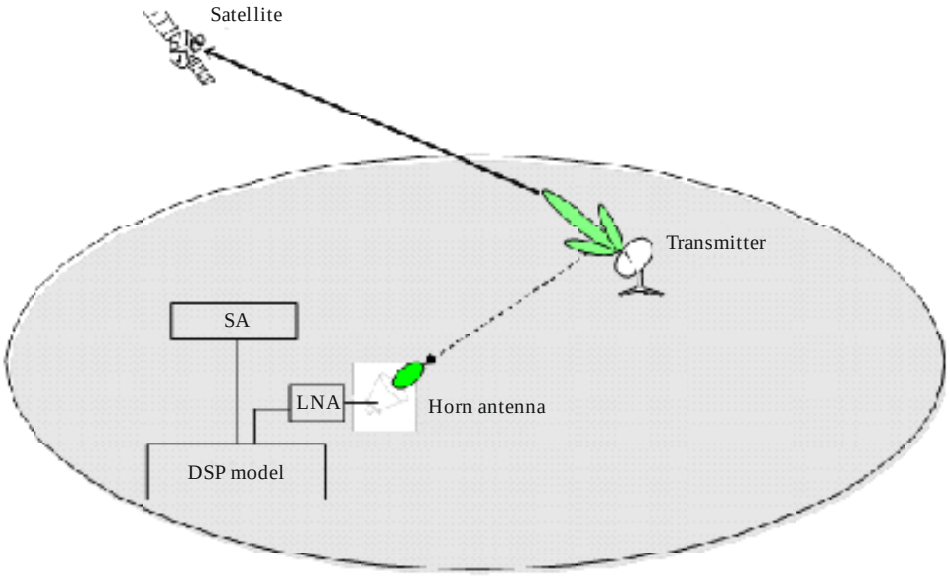

Report SM.2355-A1-05

Comparably, equipment using cyclic auto-correlation based arithmetic can detect weak signals from earth station transmitters several kilometres away, and equipment using cross-correlation based arithmetic can detect weak signals from earth station transmitters several tens of kilometres away; however equipment using a traditional monitoring receiver or spectrum analyser can only detect weak signals from earth station transmitters several hundreds of metres away under certain situations.

A1.2 Strong-signal recovery application in satellite monitoring

GSO satellite network interference happens occasionally due to equipment failure and misoperation. As a general rule, there are two signals working at overlapping frequencies. At this time strong-signal recovery may be applied for interference monitoring and alarming. A brief diagram of this application is shown in Fig. A1-6.

FIGURE A1-6

Diagram of strong-signal recovery application in satellite monitoring

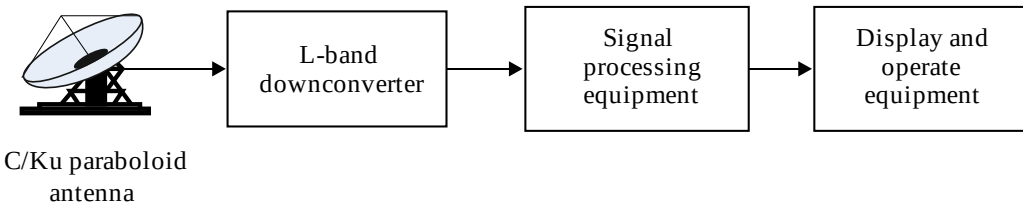

Report SM.2355-A1-0

Here is an example of a strong signal recovery application in GSO satellite network interference separation. The legal signal is in BSS application with QPSK modulation and baud-rate of 26.042 Mbit/s, the interfering signal is a CW signal.

As can be seen in Fig. A1-7 that the spectrum shown as a green line represents the received signal, which can be known as the spectrum of the mixed signal, while the spectrum in blue represents the separated interfering signal. The modulation type and the corresponding modulation parameters are listed in the form below.

FIGURE A1-7

Example of GSO satellite network interference separation

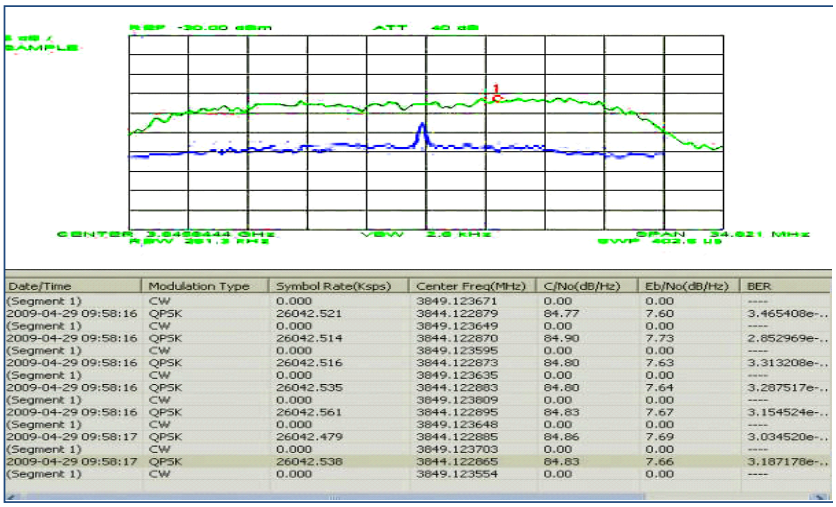

Date/Time	Modulation Type	Symbol Rate(Ksps)	Center Freq(MHz)	C/No(dB/Hz)	Eb/No(dB/Hz)	BER
(Segment 1)	CW	0.000	3849.123671	0.00	0.00	----
2009-04-29 09:58:16	QPSK	26042.521	3844.122879	84.77	7.60	3.465408e-..
(Segment 1)	CW	0.000	3849.123649	0.00	0.00	----
2009-04-29 09:58:16	QPSK	26042.514	3844.122870	84.90	7.73	2.852969e-..
(Segment 1)	CW	0.000	3849.123595	0.00	0.00	----
2009-04-29 09:58:16	QPSK	26042.516	3844.122873	84.80	7.63	3.313208e-..
(Segment 1)	CW	0.000	3849.123635	0.00	0.00	----
2009-04-29 09:58:16	QPSK	26042.535	3844.122883	84.80	7.64	3.287517e-..
(Segment 1)	CW	0.000	3849.123809	0.00	0.00	----
2009-04-29 09:58:16	QPSK	26042.561	3844.122895	84.83	7.67	3.154524e-..
(Segment 1)	CW	0.000	3849.123648	0.00	0.00	----
2009-04-29 09:58:17	QPSK	26042.479	3844.122885	84.86	7.69	3.034520e-..
(Segment 1)	CW	0.000	3849.123703	0.00	0.00	----
2009-04-29 09:58:17	QPSK	26042.538	3844.122865	84.83	7.66	3.187178e-..
(Segment 1)	CW	0.000	3849.123554	0.00	0.00	----

Report SM.2355-A1-0

A1.3 Single-channel ICA application for signal separation

Here is an example of two co-channel BPSK signals separation based on ICA algorithm. The system diagram is shown in Fig. A1-8. The two signals are with the same baud rate and only have a small carrier frequency offset. Based on the ICA algorithm, the signals are separated from the mixed signal, as shown in Fig. A1-9. If the signal-to-noise ratio (SNR) is 10 dB and the signal-to-interference ratio (SIR) is 0 dB, the correlation coefficient between the original and the separated signal could achieve more than 0.93. It can be seen clearly that the co-channel signals are completely separated. Figures A1-10 and A1-11 give the separation results in terms of a constellation diagram. By changing SNR from 4 dB to 12 dB, the bit error ratios (BERs) of the separated signals are shown in Fig. A1-12. We can see that the BERs are less than 10^{-3} when SNR is larger than 10 dB, which is a very common satellite communication environment.

In another simulation, we treat signal 1 and signal 2 as the desired signal and the interfering signal, respectively. For different SIRs (−10 dB to 10 dB), the BERs of the desired signal are shown in Fig. A1-13. We can see that the desired signal could be correctly abstracted from the mixed signal when SIRs are larger than 0 dB. For low SIRs (less than 0 dB), the interfering signal could be abstracted firstly and cancelled from the mixed signal, and then the desired could be obtained. At present, this co-channel ICA algorithm could only separate two binary digital modulation signals. More robust algorithm for multi-ary modulation signals should be studied.

FIGURE A1-8

Diagram of single-channel ICA application for signal separation

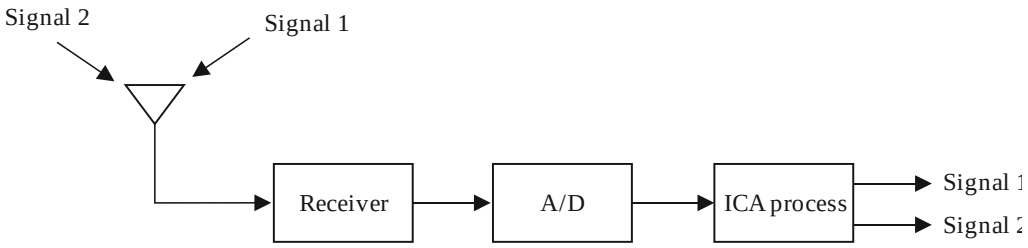

Report SM.2355-A1-0

FIGURE A1-9

Results of separation of two BPSK signals

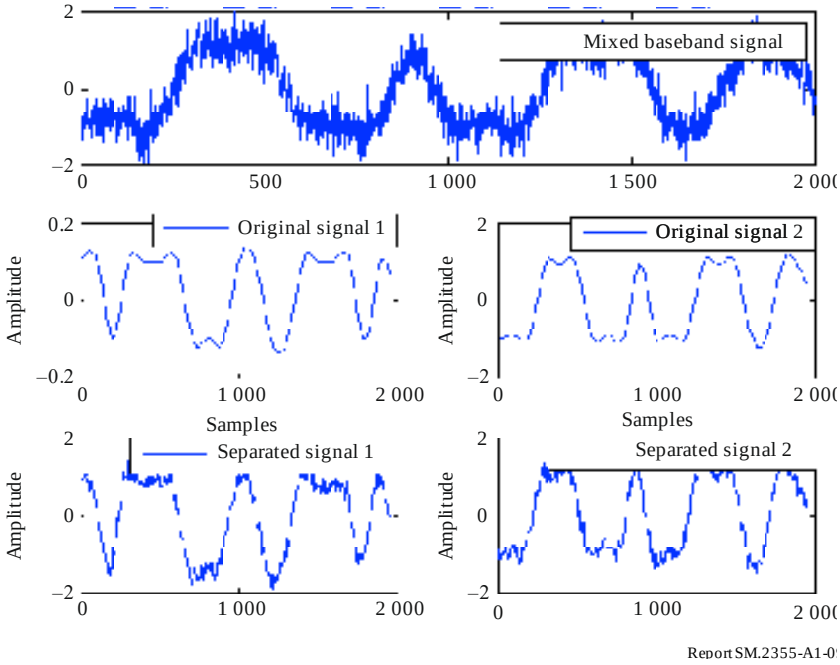

FIGURE A1-10

Constellation diagram of the mixed signal

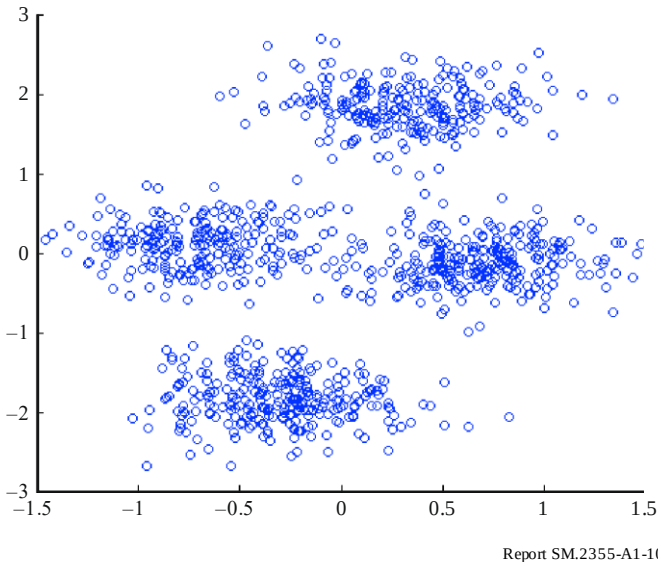

FIGURE A1-11

Constellation diagram of the separated signals

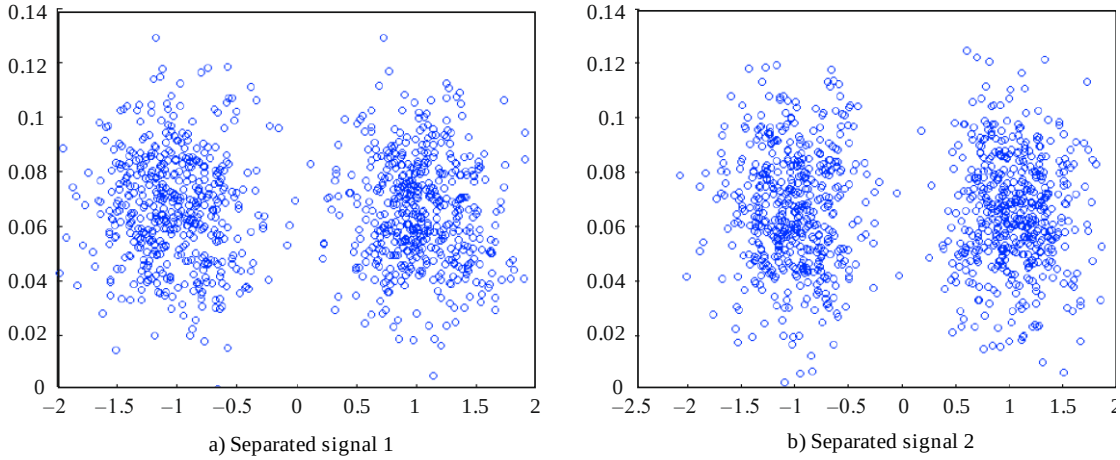

a) Separated signal 1

b) Separated signal 2

Report SM.2355-A1-11

FIGURE A1-12

BERs of the separated signals for different SNRs

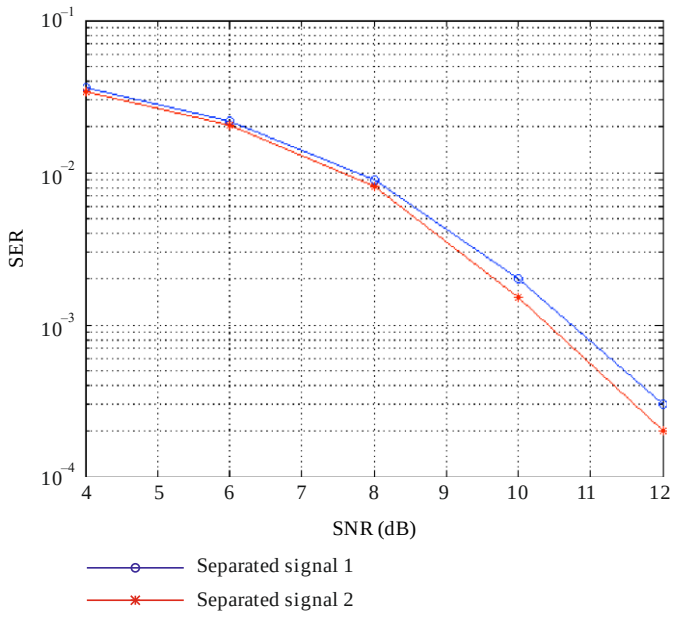

Report SM.2355-A1-12

FIGURE A1-13

BERs of the separated signal 1 for different SIRs

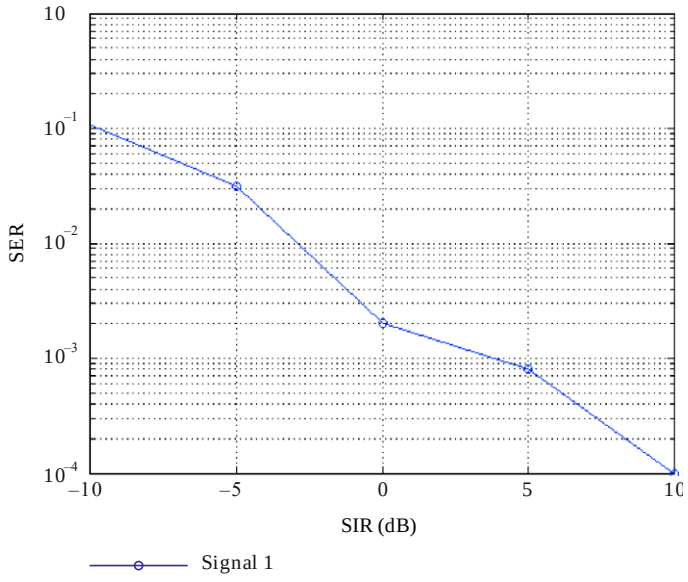

Report SM.2355-A1-1

A1.4 Spatial spectrum based beam-forming in HF/VHF monitoring

Spatial spectrum-based beam-forming technology is widely used in HF/VHF monitoring system when it is necessary to listen and locate HF/VHF signals working at overlapping frequencies. A brief structure is shown in Fig. A1-14.

FIGURE A1-14

Diagram of spatial spectrum based beam-forming application in HF/VHF monitoring

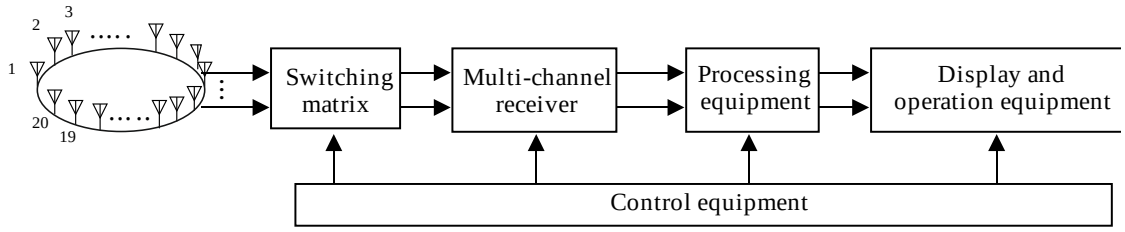

Report SM.2355-A1-1

The most common shape of array is the circular array, others are triangle and line arrays. The received signal is transmitted to a multi-channel receiver through a switching matrix. In general, the number of the receiving channels equals that of the antenna arrays. Some processing steps, such as down conversion, filtering, and digitization, are usually completed by the receiver. It is worth noting that each receiving channel should satisfy the consistence in phase and amplitude, otherwise the posterior processing would be ineffective. The processing equipment implements the direction-finding and beaming-forming algorithms, and interacts with the display and operation equipment.

The following content is an example of blind separation of two signals. Both signals are from interphone applications of FM modulation with the same power. Figure A1-15 shows the estimated result of direction of arrival by the MUSIC algorithm. It can be seen clearly that the two directions of 0° and 90° are accurately estimated. The comparison of the original and the separated signal for the desired and undesired signals are shown in Figs A1-16(a) and A1-16(b), respectively. The result

shows that both signals are well separated. By calculating *MSE* as the evaluation parameter, which is defined as:

$$MSE = \sqrt{\left(\sum_N \left(S(n) - S_e(n)\right)^2\right) / N}$$

where $S(n)$ and $S_e(n)$ are the original and the separated signal respectively, N is the number of the signal, and the magnitude of *MSE* is around 10^{-3}.

FIGURE A1-15

Results of the direction of arrival estimation

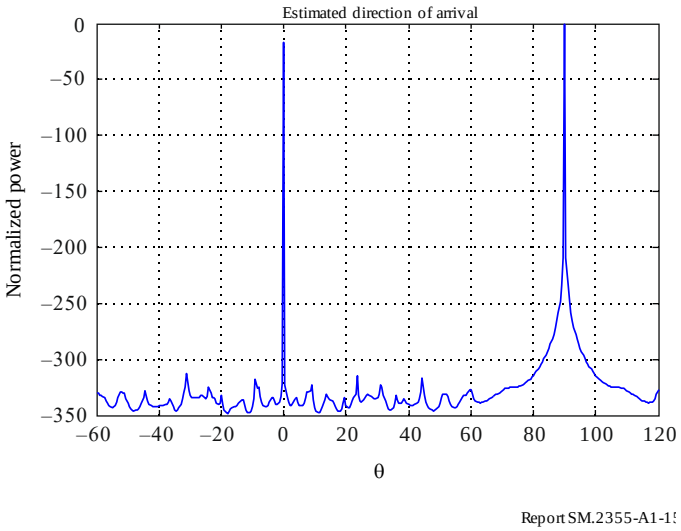

FIGURE A1-16

Comparison between the original and the separated signal

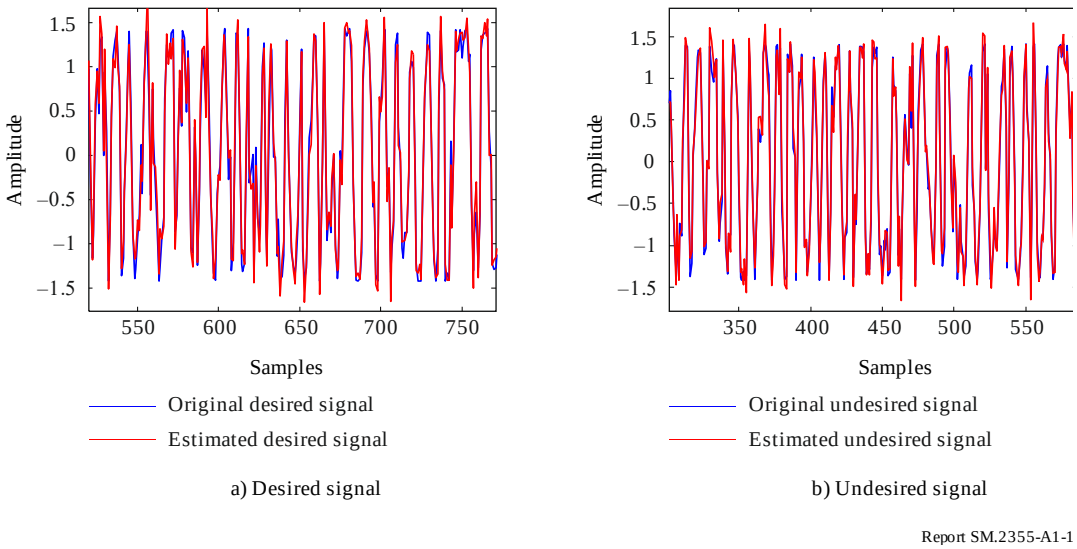

Figure A1-17 shows the evaluation result of the *MSE* ratio under different power ratio between the desired and undesired signals. It can be seen that the power ratio has significant influence on the effect of the separation result. Generally speaking, strong signal outcomes a comparable less *MSE* than that of the weak signal, and shows a better separation performance. As a particular case, the *MSE*s are similar when the two signals have the same power.

FIGURE A1-17

***MSE*s under different power ratios between the desired and undesired signals**

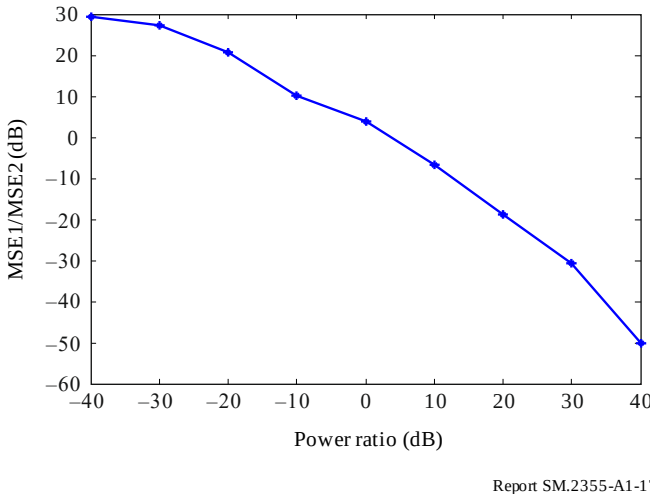

A1.5 Multi-channel ICA application for signal separation

This part introduces the results of evaluation of multi-channel ICA application for interference signal separation using an experimental test bed.

A1.5.1 Details of tests

A signal comprising an interference wave superimposed on a desired signal was transmitted as the test signal, which was then received by an array antenna. The received signal was first A/D converted and then the ICA processing was carried out.

By obtaining the difference between the estimated power ratio (DUR_{est}) of the desired wave and the interference wave which were separated by ICA processing and the set electric power ratio (DUR) of the test signal, the DUR estimation accuracy was evaluated.

Desired to undesired power ratio of the test signal (DUR) = (desired signal power)/(undesired signal power)

Estimated power ratio after ICA processing (DUR_{est})

$$= (\textit{desired signal power}) / (\textit{undesired signal power})$$

DUR estimation accuracy (A) = $DUR_{est} - DUR$

As viewed from the array antenna, the arrival direction of the desired wave is kept fixed, the arrival direction of the interference wave is changed from 5° to 180°, and the change in the DUR estimation accuracy due to changes in DUR for each arrival angle were evaluated.

Figure A1-18 shows a system diagram of the evaluation test.

FIGURE A1-18

System diagram of evaluation test

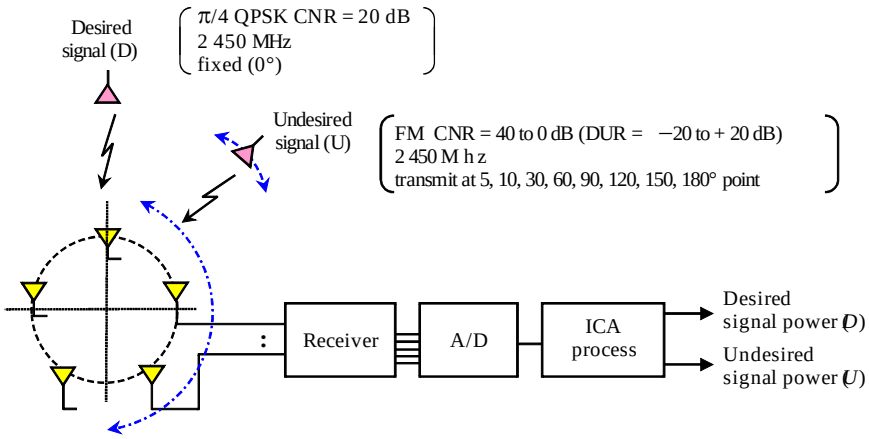

A1.5.2 Test results

A constellation diagram of the received signal before ICA processing and the desired wave and interference wave separated by ICA processing is shown in Fig. A1-19. Furthermore, the measured results of the DUR estimation accuracy in the case of the desired wave π/4 QPSK and the interference wave FM are shown in Fig. A1-20.

In the range of DUR = −15 to +10 dB, it was confirmed that it is possible to estimate the DUR of the interference signal within an accuracy of less than 2 dB.

With the same procedure as this test, we carried out a test in the case of the test signal comprising the desired wave AM and the interference wave FM. Although there was some slight difference in the results, results showed on the whole a similar trend and similar results.

With the same procedure as this test, the results of carrying out tests for antenna aperture diameters showed the trend that the range of DUR that can be measured becomes wider towards larger aperture diameters.

FIGURE A1-19

Constellation diagram of signals separated by ICA

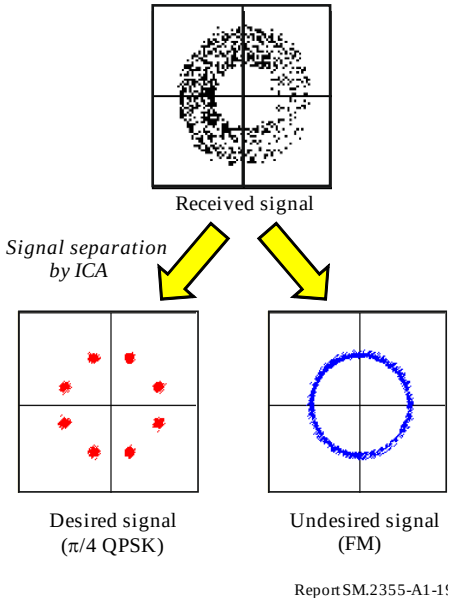

FIGURE A1-20

Accuracy of DUR estimation

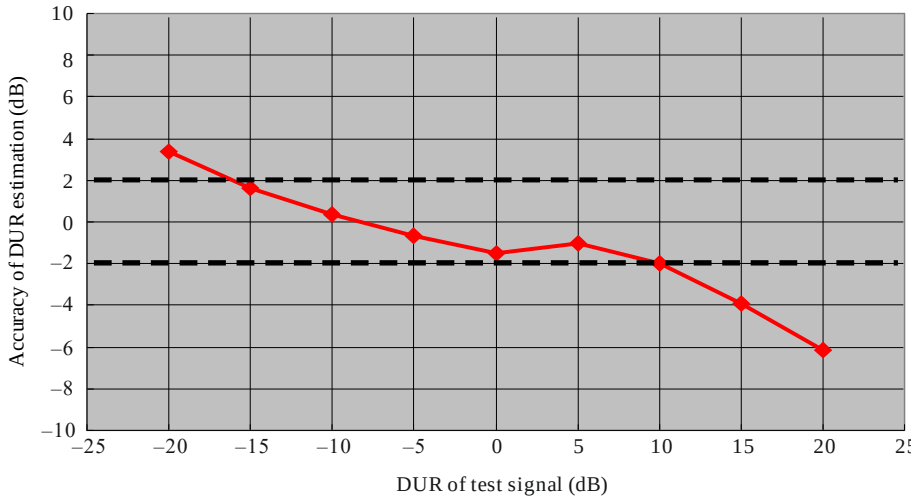

A1.5.3 Interference detection processing

As shown in the results of evaluating the ICA method, this method can estimate DUR with a high accuracy from the signal power ratio after separation. Therefore, it is evident that it is possible to monitor quantitatively and with appropriate timing in actual situations of weak levels of interference in which there is no significant degradation in the communication quality, and in rarely occurring actual cases of interference.

In more specific terms, in a general digital wireless system, even when there is an interference of about *DUR* = 10 dB, by the use of error correction codes, the user does not notice that interference has occurred. Because of quantitatively estimating the DUR using the ICA method, it is considered possible to take countermeasures before a significant degradation occurs in the communication quality.

As shown in Fig. A1-21, in this method, in the range of *DUR* = −15 to +10 dB, since it is possible to measure the signal level with an accuracy of ±2 dB, within this DUR range, it is expected to be possible to detect the presence of an interference with a good accuracy.

By setting the threshold value for detecting the presence of an interference by referring to the *C/N* (= *DUR*) required by the communication system of the desired wave, it is possible to output an alarm or make a record automatically in synchronization with the interference detection timing.

A1.6 GSM base station geolocation

It is necessary to locate GSM base stations when there is interference between different GSM network operators, or there is demand on GSM network coordination at border areas. Monitoring stations can be used to differentiate GSM base stations belonging to different GSM network operators by utilizing traditional DF and geolocation method. However, it is easier to implement such a task by decoding GSM signals and extracting information, such like GSM network operator, Cell Global Identification (CGI), etc.

CGI is a unique number used to identify the GSM base station the user equipment is connected to. The Cell Global Identification is the concatenation of the Location Area Identification and the Cell Identity. The brief diagram of extracting CGI is shown in Fig. A1-23.

FIGURE A1-21

Diagram of extracting cGI

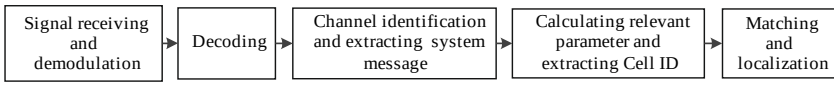

Report SM.2355-A1-2

GSM signal should be demodulated and decoded firstly after it is received by a monitoring station receiver. Then the special channel should be identified and the system message should be extracted from it. Position of GSM base station can be known after matching relevant parameter and cell ID with database. In combination with AOA method, a mobile monitoring station can locate accurate position of GSM base stations in one area by planning appropriate monitoring route.

Annex 2

Examples of the application of combined geolocation

A2.1 Hybrid AOA/TDOA

In general, there is no single method such as the ones based on measuring time difference of arrival (TDOA) and angle of arrival (AOA) that will provide accurate location estimation under all circumstances. Each method has its own advantages and limitations in terms of location accuracy.

TDOA location methods generally provide better location accuracy for wideband signals than the AOA-based location method. However, the TDOA-based methods require relatively more stations than the AOA-based methods to perform location of emitters. For instance, the TDOA-based methods require at least three properly distributed stations for location. The AOA methods, on the other hand, require two stations for location. However, a small error in the angle measurements will result in a large location error if the station is far away from the transmitter. Therefore, to achieve better location accuracy, a combination of two or more location schemes should be considered in order to complement each other.

The location is performed by processing the information available from each station, including AOA measurements, TDOA measurements and station position information. Combining the AOA method with the TDOA method (called hybrid AOA/TDOA) can assist in eliminating location ambiguity associated with TDOA alone and can enhance location accuracy. This is illustrated in Fig. A2-1. A more complete discussion of Hybrid AOA/TDOA methods is contained in the ITU Handbook on Spectrum Monitoring, Edition 2011, Chapter 4, § 4.7.3.6.

FIGURE A2-1

Improved results based on AOA/TDOA combined techniques

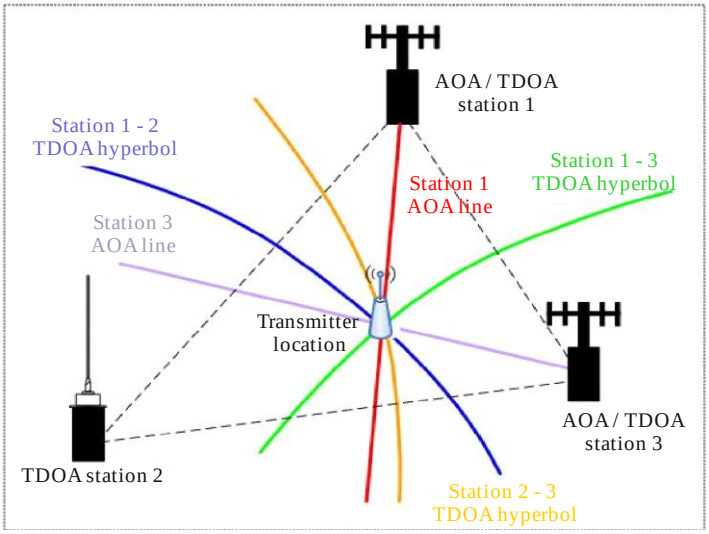

Report SM.2355-A2-01

Using POA techniques generally works best at specific distances from the transmitter depending on power and what clutter and other signal disturbances (e.g. absorbers) are in the area. This is especially important since these techniques typically use line-of-sight propagation models, working as a combined geolocation technique along with AOA and TDOA. This is illustrated in Fig. A2-2.

FIGURE A2-2

Combined geolocation

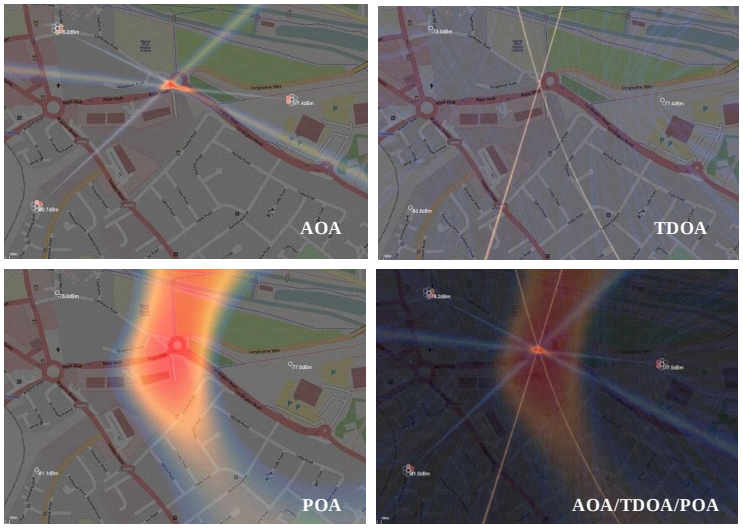

Report SM.2355-A2-0

A2.2 Hybrid TDOA/GROA

A2.2.1 Introduction

Grid monitoring network technology is one of the technologies which can spatially describe and display unknown radio emitters and assess spectrum resources using remote distributed RF intelligent monitoring nodes. The grid monitoring network technology meets the challenges of modern spectrum usage and efficiency requirements of managing spectrum resources for the metropolitan environment. The components and architecture of this type of system differentiate it from other systems with more traditional angle-of-arrival direction-finding (DF) systems, which can be more complex, expensive and often used in large-scale scenarios.

China commissioned a study into the design of a grid monitoring network that could be deployed in large numbers to automatically detect, identify and locate the source of interfering radio signals over a large part of a metropolitan area in China. In June, 2012, the experimental programme was launched, which covers over 75 square kilometres in the downtown area of Shanghai with 46 networkable nodes, as shown in Fig. A2-3. More than 50 researchers and engineers joined this programme, which is the first experimental area to explore methods for metropolitan area radio monitoring with a large number of cost-effective nodes in China. The experimental programme was implemented in June 2013. The field test was conducted by 16 test participants from third parties in August 2013. The experimental network had been running in the test phase for nearly one year by 2014.

FIGURE A2-3

The grid monitoring network with 46 nodes

Report SM.2355-A2-0

A2.2.2 Architecture of grid monitoring network

The grid monitoring network is a typical mesh network that supports dynamic networking and scalable structure. The structure of the grid monitoring network in the programme consists of three layers, as shown in Fig. A2-4:

– the sensor layer: including all the cost-effective networkable nodes (bi-conical antenna, sensor and GPS antenna);

– the middle service layer: consisting of the sub-centre servers with several grids, to organize and allocate the monitoring tasks to the sensors;

– the monitoring centre layer: including all the software applications such as spectrum monitoring, locating and data mining.

FIGURE A2-4

The architecture of the grid monitoring network

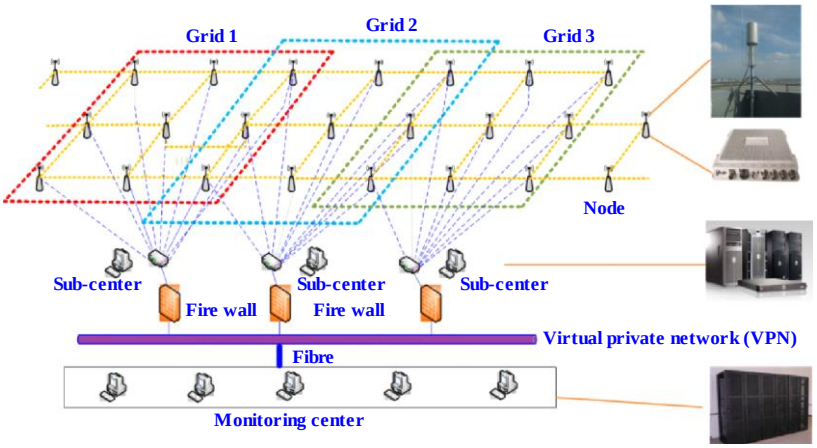

The grid monitoring network process flow is shown in Fig. A2-5.

FIGURE A2-5

The grid monitoring network process flow

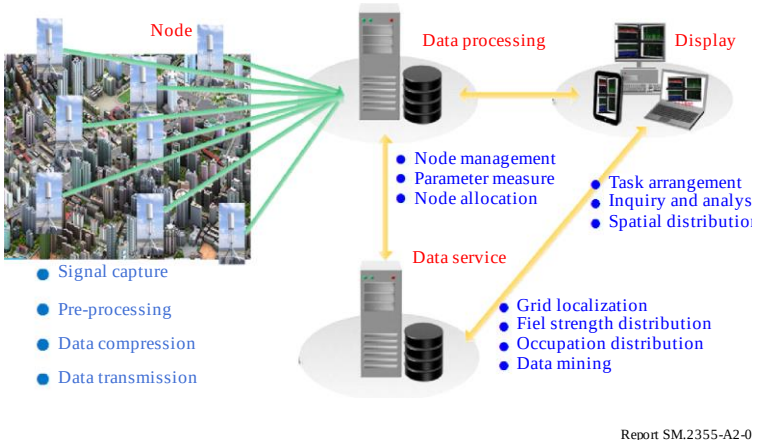

A cost-effective networkable node, such as that shown in Fig. A2-6, is the key component in the grid monitoring network. It is significantly different from the direction finding node, which is often multi-channels and quite expensive. Therefore, the grid monitoring network costs may be significantly lower by utilizing signal correlation methods, depending on the size of the monitoring area and hence the number of required nodes. Investigation of cost is of great importance for developing countries with a limited budget, and to metropolitan areas with large number of monitoring nodes.

FIGURE A2-6

Cost-effective networkable RF sensor and bi-conical antenna

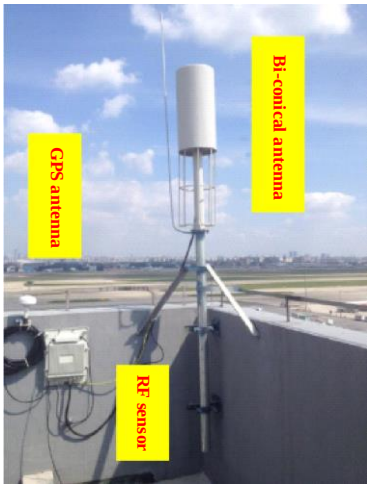

Report SM.2355-A2-0(

A2.2.3 System functionalities

A2.2.3.1 Intercept weak signal

The monitoring performance has been tested based on the mounted sensors from the grid monitoring network. The field test has been carried out as long as 19 days in the coverage areas by 16 testers from third parties.

The minimum emission power level of the "target" emitter (emitter to be detected) is defined as signal-to-noise ratio (SNR) ≥ 6 dB in the receiver for different frequencies (including 115 MHz, 320 MHz, 575 MHz, 965 MHz, 1 300 MHz, 1 700 MHz, 2 600 MHz) and different bandwidths (including 12.5 kHz, 25 kHz, 100 kHz, 200 kHz, 1.25 MHz, 8 MHz), the result is shown as Table A2-1.

TABLE A2-1

Detection probability for different power of the emitter (131 measurements)

	Power emitter ≥ 1W	**Power emitter ≥ 0.1W**	**Power emitter ≥ 0.05W**
Detection measurements (SNR ≥ 6 dB)	128	114	92
Detection probability (SNR ≥ 6 dB)	97.7%	87%	70.2%

A2.2.3.2 Hybrid geolocation

The grid geolocation (hybrid TDOA and GROA: time difference of arrival and gain ratio of arrival) performance has been tested.

The gain ratio of arrival (GROA) is an energy-based passive method that can be used to estimate the positions of the source from the multiple sensors. This method does not require accurate time synchronization between sensors. A particular value of the GROA estimate defines a circle between the two receivers on which the radio transmitter may exist.

The time difference of arrival (TDOA) technique is one of the most promising position location techniques for wireless communication systems. TDOA techniques are based on estimating the difference in the arrival times of the signal from the source at multiple receivers. A particular value of the time difference estimate defines a hyperbola between the two receivers on which the radio transmitter may exist, assuming that the source and the receivers are coplanar, shown as Fig. A2-7.

FIGURE A2-7

Schematic diagram of the hybrid GROA/TDOA geolocation techniques

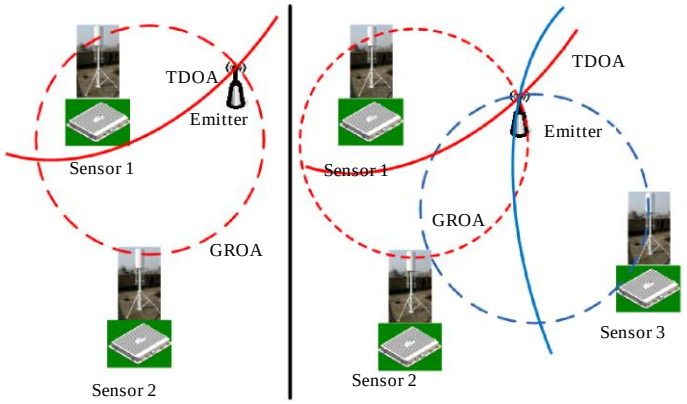

The test result shows that the proportion of typical errors (deviation between the true location and estimated one) less than 300 metres is about 82.3% in the 402 measurements. The proportion to the typical value of the grid locating deviations less than 100 metres is about 24.9%. Table A2-2 shows the parameters of the testing transmitter.

Specifically, the grid monitoring network can distinguish and geolocate two signals operating on the same frequency simultaneously because of the grid resolution. For a test example with two emitters with following parameters as frequency 220 MHz, bandwidth 50 kHz, power 1 W and QPSK modulation, the grid monitoring network gives high spatial resolution for simultaneous emitters operating at different distances apart from each other (in Figs. A2-8, A2-9 and A2-10), except in the case where the two emitters are in the same grid (in Fig. A2-11).

TABLE A2-2

Hybrid geolocation test parameters

Parameters	Value
Frequency (MHz)	115, 320, 575, 965, 1 300, 1 700, 2 600
Bandwidth (Hz)	12.5K, 25K, 100K, 200K, 1.25M, 8M
Modulation	AM, FM, FSK, QPSK, MSK, QAM
Power	1W

FIGURE A2-8

Co-frequency signals spatial separation (Emitter pairwise distance is 7.2 km)

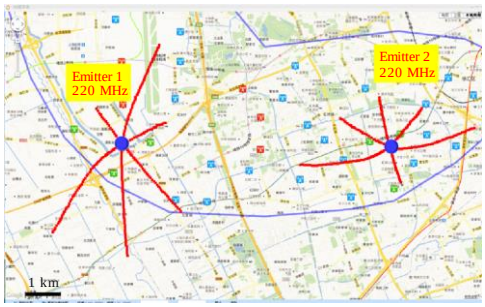

Report SM.2355-A2-0

FIGURE A2-9

Co-frequency signals spatial separation (Emitter pairwise distance is 5.7 km)

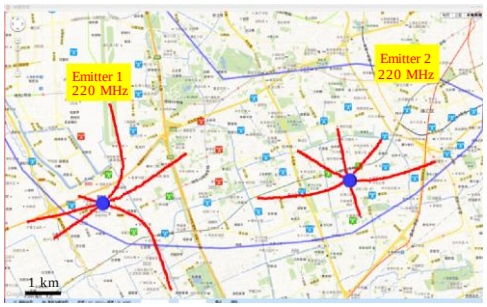

Report SM.2355-A2-0

FIGURE A2-10

Co-frequency signals spatial separation (Emitter pairwise distance is 4.1 km)

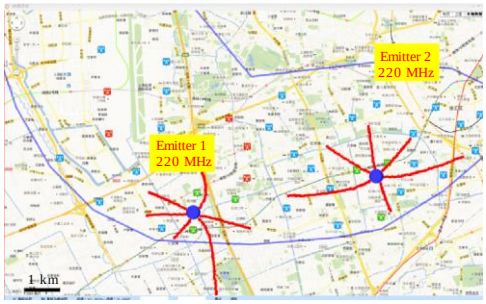

Report SM.2355-A2-1

FIGURE A2-11

Co-frequency signals spatial separation (Emitter pairwise distance is 0.6 km)

Report SM.2355-A2-1

A2.2.3.3 Field-strength distribution

Field strength can be measured by all nodes simultaneously, and the distribution of the channel in the coverage area can be detected and calculated by the grid monitoring network by real-time data interpolation. The distribution is computed according to the field strength detected by all the sensors, and the monitoring data will be merged in real-time. Two examples are presented below for the case of one 3 W emitter and two 3 W emitters operating simultaneously.

FIGURE A2-12

Field strength distribution (Frequency 140.5 MHz, bandwidth 12.5 KHz, FM, power 3W)

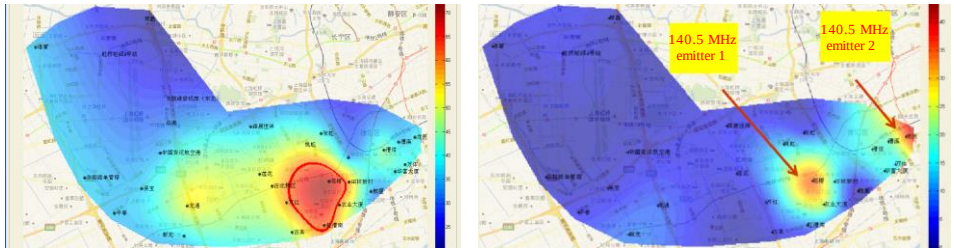

a) Single walkie-talkie test

b) Double walkie-talkie test

Report SM.2355-A2-12

Figure A2-12 shows that the radio propagation is anisotropic apparently in metropolitan environments, which is different from the theoretical isotropic propagation models. The two emitters operating on the same frequency can be spatially distinguished clearly by the grid monitoring network. Here, the distance between the emitters is less than 3 km. However, this is difficult to accomplish using a more conventional DF network system in the metropolitan environment.

A2.2.3.4 Geographic occupation and electromagnetic radiation distribution

Traditional spectrum occupancy is often a single value for one place. Also, it is not easy to describe clearly how spectrum resources are used. The grid monitoring network can provide details about the spectrum occupation spatially. The spectrum occupancy can be measured by all the nodes simultaneously in Fig. A2-13 (Freq = 400.5 MHz, BW = 12.5 kHz, FM, power = 3 W).

With the raw spectrum data within the grid monitoring network, the electromagnetic radiation geographic distribution can also be described in the covered areas, as shown in Fig. A2-14. The frequency band is 30 MHz to 3 000 MHz, and the unit of the electromagnetic radiation is power density in uW/cm^2.

FIGURE A2-13

Geographical spectrum occupancy distribution

Report SM.2355-A2-13

FIGURE A2-14

Electromagnetic radiation distribution

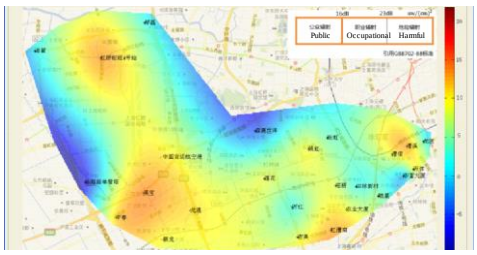

Report SM.2355-A2-14

A2.2.4 Conclusion

The grid monitoring network with cost-effective nodes has the ability to intercept the weak signals, to provide the details of radio monitoring and to describe the spectrum spatial distribution for the metropolitan environment, so it is meaningful and effective in identifying the spectrum spatial distribution and the location of the interference sources quickly.

List of abbreviations

LIA	Locked-in amplifier
HOS	Higher order statistics
SCD	Spectral correlation density
CDMA	Code division multiple access
OFDM	Orthogonal frequency division multiplexing
ANC	Adaptive noise cancelling
PSK	Phase shift keying
QAM	Quadrature amplitude modulation
LMS	Least mean square
RLS	Recursive lease square
AWGN	Additive white Gaussian noise
MUSIC	MUtiple SIgnal Classification
DSP	Digital signal processing
AOA	Angle of arrival
TDOA	Time difference of arrival
FDOA	Frequency difference of arrival
POA	Power of arrival